
MAGNETO-ACOUSTO-ELECTRIC TOMOGRAPHY WITH MAGNETIC FIELD MEASUREMENTS: MODELING, INVERSION AND STABILITY

A PREPRINT

Lingyun Qiu^{1,2}, Siqin Zheng³

¹ Yau Mathematical Sciences Center, Tsinghua University, Beijing 100084, China

² Yanqi Lake Beijing Institute of Mathematical Sciences and Applications, Beijing 101408, China
(lyqiu@tsinghua.edu.cn)

³ Department of Mathematical Sciences, Tsinghua University, Beijing 100084, China
(zhengsq21@mails.tsinghua.edu.cn)

March 3, 2026

ABSTRACT

Magneto-acousto-electric tomography (MAET) combines ultrasound with a static magnetic field to infer the electrical conductivity of an object. In this paper, we present a rigorous quasi-static mathematical model for MAET with magnetic field measurements and introduce an adjoint problem to decouple the resulting hybrid inverse problem. This yields a two-step inversion procedure: solving an acoustic inverse source problem and then recovering the conductivity from an internal current density. We prove that, under explicit smallness assumptions on the conductivity and coil geometry, the conductivity can be recovered with Lipschitz stability in both bounded and half-space geometries.

Keywords Inverse problems · Coupled-physics imaging · Magnetic field measurements · Quasi-static modeling · Conditional stability

MSC Classification 35J25 · 35R30 · 65N21 · 92C55

1 Introduction

In clinical diagnosis and pathological research, electrical conductivity is a crucial physical property of biological tissues for distinguishing between normal and pathological tissues. Therefore, conductivity imaging plays a critical role in medical imaging.

In mathematics, an imaging problem is typically modeled as an inverse problem, and the imaging resolution depends on the stability of the corresponding inverse problem. The conventional method, electrical impedance tomography (EIT), has low resolution because its inverse problem exhibits only logarithmic stability [43]. This means that errors in data are significantly amplified during the inversion procedure, resulting in highly inaccurate reconstructions. To achieve more accurate conductivity inversion, various coupled-physics imaging methods have been developed in recent years. These methods combine the electrical process with other processes such as acoustics and magnetism, utilizing observable signals generated by their interaction, such as acousto-electric effect and electromagnetic induction, to reconstruct the conductivity. The inverse problems of these methods typically demonstrate better stability, often of a Hölder or even Lipschitz type, leading to higher resolution. For detailed introductions on coupled-physics imaging, we refer to [45] and the references therein.

A specific modality of coupled-physics imaging method, known as magneto-acousto-electric tomography (MAET), is designed based on the Hall effect, where vibrating charged particles in a magnetic field are subjected to the Lorentz force, thereby generating electromagnetic signals. When first proposed, MAET relied on measurements of the induced

voltage on the boundary of the imaging object [19, 38, 44]. Kunyansky develops a rigorous and general mathematical model and an almost explicit inversion procedure [31]. One of the key steps, recovering the conductivity from internal current densities, requires suitable design of boundary conditions to generate linearly independent current densities. A potential approach is explored in [37], where local Lipschitz stability results are derived for both full data and partial data. Kunyansky et al. also consider other settings for better applications [32, 33]. As a noninvasive technique that does not involve ionizing radiation, MAET poses fewer risks than traditional X-ray imaging and thus holds promise for clinical applications.

More recently, measurements of the induced electromotive force (emf) in coils placed outside the object have been investigated [18, 46, 47]. See Figure 1 for a simple experimental setup. This variant is referred to as MAET with magnetic field measurements, since by Faraday’s law, the measured emf in a coil corresponds to the rate of change of the magnetic flux through its bounding surface. Compared to the boundary measurements using electrodes, this contactless approach avoids the problems caused by contact impedances and the screening effect of superficial insulating layers such as skin and bone [15, 41]. It also eliminates patient discomfort in clinical diagnosis.

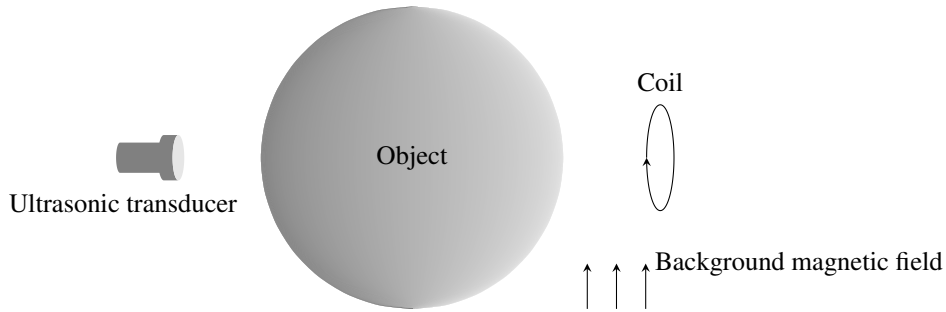


Figure 1: A simple experimental setup of MAET with magnetic field measurements

Existing models of MAET with magnetic fields measurements are based on the Maxwell’s system under simplifying approximations, such as neglecting displacement currents and assuming low conductivity, which lack rigorous mathematical justification. These simplifications, while useful for initial experimental validation [16, 23, 42], restrict the imaging resolution, reliability, and clinical applicativity. Therefore, establishing a rigorous mathematical foundation is essential to advance this technique by properly decoupling the interacting physics and guiding experimental designs for stable reconstruction. This work aims to fill this gap by developing a rigorous model and inversion framework, analogous to MAET with voltage measurements [31]. Additionally, we analyze the stability of conductivity reconstruction, offering insights into appropriate configurations of detection coils.

The inverse problem of a coupled-physics imaging technique can typically be decoupled into two steps: first, reconstructing some internal functionals or vector fields from boundary or external measurements; second, using these to recover the unknown coefficients. Further examples and details can be found in [4, 10] and the references therein. The inversion procedure of MAET with voltage measurements, as developed in [31], conforms to this paradigm.

Regarding MAET with magnetic field measurements, since the underlying principle is similar, we aim to follow this framework. We adopt a quasi-static model of the Hall effect instead of the full Maxwell’s system, because the electromagnetic induction happens much more rapidly than ultrasonic propagation. This significant difference in time scales plays a crucial role in the decoupling process and inversion procedure. A stationary adjoint equation is introduced, enabling the decoupling of the hybrid inverse problem into an inverse source problem for the acoustic wave equation and an inverse medium problem for the electrostatic equation with internal data. The first problem is analogous to that in MAET with voltage measurements, whereas the second does not admit an explicit reconstruction formula. We use a multiplier approach to derive some stability results, which require a nonzero constraint on the data. External coils offer more flexibility and promise compared to the boundary conditions considered in [3, 4, 37], as they provide additional degrees of freedom for data generation. However, despite the potential, designing coils that satisfy the nonzero constraint remains an underexplored challenge. This paper presents an initial analysis of coil configurations based on the imaging domain and some prior knowledge of the unknown conductivity.

This paper is structured as follows. Section 2 introduces the quasi-static model of MAET with magnetic field measurements and relevant preliminaries. Section 3 develops the inversion procedure. Section 4 addresses the key challenge of stabilizing conductivity reconstruction from an internal current density, providing conditional stability results for both bounded domains and half-space. Concluding remarks are presented in Section 5.

2 Mathematical model

Since the time scales of the ultrasonic and electromagnetic processes differ by orders of magnitude [5], we model the forward problem of MAET in a quasi-static manner instead of using the full Maxwell's equations. Specifically, at any given instant during the acoustic wave propagation, the electromagnetic induction in the space can be regarded as nearly instantaneous, and therefore the overall process can be effectively treated using a quasi-static approximation as in [31].

Denoting the imaging object by a domain Ω in \mathbb{R}^3 , MAET aims to reconstruct the conductivity $\sigma(x)$, which is a spatial function in Ω . In the MAET experiments, the object is placed in a static magnetic field with constant magnetic induction intensity B_0 . When an acoustic wave is transmitted, it propagates through the object and causes the charged particles inside to vibrate with velocity $V(x, t)$. The arising Lorentz force leads to the flow of charged particles, i.e., the Lorentz current $\sigma(x)V(x, t) \times B_0$. At each time instant t , an electric potential $u(x, t)$ is instantaneously induced within the object, with a secondary current $-\sigma(x)\nabla u(x, t)$. Due to charge conservation and the instantaneous redistribution of charges within the imaging object, the total current density $J = \sigma V \times B_0 - \sigma \nabla u$ is divergence-free. Furthermore, since the object is typically surrounded by an insulating medium such as air, the total current J does not flow out through the boundary. These physical considerations lead to the following Neumann problem for the potential u :

$$\begin{cases} \nabla \cdot (\sigma \nabla u) = \nabla \cdot (\sigma V \times B_0) & \text{in } \Omega, \\ \partial_\nu u = V \times B_0 \cdot \nu & \text{on } \partial\Omega, \end{cases} \quad (2.1)$$

where ν denotes the unit outer normal direction on the boundary $\partial\Omega$. According to the Biot-Savart law of magnetostatics, the total current J generates a magnetic field with flux density

$$B(y, t) = \frac{\mu}{4\pi} \int_{\Omega} J(x, t) \times \frac{y - x}{|y - x|^3} dx \quad (2.2)$$

in the whole space \mathbb{R}^3 , where the permeability μ is assumed as the constant of vacuum. For any external coil L , the measured time-varying induced emf is, according to Faraday's law of induction, the negative rate of change of the magnetic flux through any surface D bounded by L :

$$m_L(t) = -\frac{d}{dt} \int_D B(y, t) \cdot n(y) dS_y = -\frac{\mu}{4\pi} \int_{\Omega} \partial_t J(x, t) \cdot \int_D \frac{(y - x) \times n(y)}{|y - x|^3} dS_y dx. \quad (2.3)$$

Here n denotes the unit normal vector to the surface D . Its direction is chosen to be compatible with the orientation of L via the right-hand rule.

The aim of MAET with magnetic field measurements is to reconstruct the conductivity σ in Ω , from $m_L(t)$ for several coils L , under different background field B_0 and ultrasonic excitation $V(x, t)$.

Denoting

$$C_L(x) = -\frac{\mu}{4\pi} \int_D \frac{(y - x) \times n(y)}{|y - x|^3} dS_y = -\frac{\mu}{4\pi} \nabla \times \int_D \frac{n(y)}{4\pi|y - x|} dS_y, \quad (2.4)$$

which totally depends on the coil L and is time-independent, the measurement (2.3) can be written as

$$m_L = \int_{\Omega} \sigma(\partial_t V \times B_0 - \nabla v) \cdot C_L dx, \quad (2.5)$$

where $v = \partial_t u$ solves the Neumann problem

$$\begin{cases} \nabla \cdot (\sigma \nabla v) = \nabla \cdot (\sigma \partial_t V \times B_0) & \text{in } \Omega, \\ \partial_\nu v = \partial_t V \times B_0 \cdot \nu & \text{on } \partial\Omega. \end{cases} \quad (2.6)$$

Now we introduce the following adjoint problem

$$\begin{cases} \nabla \cdot (\sigma \nabla w_L) = \nabla \cdot (\sigma C_L) & \text{in } \Omega, \\ \partial_\nu w_L = C_L \cdot \nu & \text{on } \partial\Omega, \end{cases} \quad (2.7)$$

so that the second part in (2.5) can be rewritten by integration by parts into

$$\int_{\Omega} \sigma \nabla v \cdot C_L dx = \int_{\Omega} \sigma \nabla v \cdot \nabla w_L dx = \int_{\Omega} \sigma \partial_t V \times B_0 \cdot \nabla w_L dx.$$

Therefore,

$$m_L = \int_{\Omega} \sigma \partial_t V \times B_0 \cdot (C_L - \nabla w_L) dx = \frac{B_0}{\rho} \cdot \int_{\Omega} J_L \times \nabla p dx, \quad (2.8)$$

where $J_L = \sigma(C_L - \nabla w_L)$ is the total current density of the adjoint problem (2.7) (called the adjoint current for short in the following), and p is the acoustic pressure satisfying

$$(\partial_t^2 - c^2 \Delta)p = 0, \quad \partial_t V = \frac{1}{\rho} \nabla p$$

with sound speed c and mass density ρ regarded as known constants.

Before investigating how to recover the conductivity σ from these measurements, we introduce some necessary notations and preliminaries on the adjoint problem (2.7).

2.1 Notations

During estimates, we use the symbol C to denote positive constants with their dependence in parentheses.

For $k \in \mathbb{N}$ and a domain $\Omega \subset \mathbb{R}^d$, we use the standard notation $C^k(\overline{\Omega})$ to denote the space of k -times continuously differentiable functions on $\overline{\Omega}$, with the norm

$$\|u\|_{C^k(\overline{\Omega})} = \max_{|\beta| \leq k} \sup_{x \in \overline{\Omega}} |\partial^\beta u(x)|.$$

For $\alpha \in (0, 1]$, we denote by $C^{k,\alpha}(\overline{\Omega})$ the Hölder space consisting of $u \in C^k(\overline{\Omega})$ whose k -th partial derivatives are Hölder continuous with exponent α , that is,

$$[\partial^k u]_{\alpha;\Omega} = \max_{|\beta|=k} \sup_{\substack{x,y \in \overline{\Omega} \\ x \neq y}} \frac{|\partial^\beta u(x) - \partial^\beta u(y)|}{|x - y|^\alpha} < \infty,$$

with the norm

$$\|u\|_{C^{k,\alpha}(\overline{\Omega})} = \|u\|_{C^k(\overline{\Omega})} + [\partial^k u]_{\alpha;\Omega}.$$

We say $\partial\Omega \in C^{k,\alpha}$ if each point of $\partial\Omega$ has a neighborhood in which $\partial\Omega$ is the graph of a $C^{k,\alpha}$ function of $d - 1$ of the coordinates. We use $C_c^\infty(\Omega)$ to denote the space of smooth functions with compact supports in Ω .

For $p \in [1, \infty]$, we use the notation $W^{k,p}(\Omega)$ for the L^p -based Sobolev space of k -th order, i.e.

$$W^{k,p}(\Omega) = \{u \in L^p(\Omega) : \partial^\beta u \in L^p(\Omega), \forall |\beta| \leq k\},$$

with the norm

$$\|u\|_{W^{k,p}(\Omega)} = \sum_{|\beta| \leq k} \|\partial^\beta u\|_{L^p(\Omega)}.$$

When $p = 2$, the space $W^{k,2}(\Omega)$ is usually abbreviated as $H^k(\Omega)$. In general, we introduce the fractional Sobolev space

$$H^s(\mathbb{R}^d) = \{u \in L^2(\mathbb{R}^d) : (1 + |\xi|^2)^{s/2} \hat{u}(\xi) \in L^2(\mathbb{R}^d)\}$$

for $s > 0$, with the norm

$$\|u\|_{H^s(\mathbb{R}^d)} = \|(1 + |\xi|^2)^{s/2} \hat{u}\|_{L^2(\mathbb{R}^d)},$$

where \hat{u} is the Fourier transform of u . When the boundary $\partial\Omega \in C^{0,1}$ (usually called Lipschitz), the space $H^s(\partial\Omega)$ is defined via local charts for $s \in (0, 1)$. In this paper, we only need the space $H^{1/2}(\partial\Omega)$, which is actually the space of traces of $H^1(\Omega)$ and the trace theorem shows that

$$\|u\|_{H^{1/2}(\partial\Omega)} \leq C(d, \Omega) \|u\|_{H^1(\Omega)} \quad (2.9)$$

Its dual space is defined as $H^{-1/2}(\partial\Omega)$, and the duality pair between them is denoted by $\langle \cdot, \cdot \rangle_{\partial\Omega}$. For more details about Sobolev spaces, see [1] and [13, Chapter 5]. For simplicity, we do not distinguish the notation between (scalar) functions (usually denoted by lowercase letters) and vector fields (usually denoted by uppercase letters).

For $\Omega \subset \mathbb{R}^3$, we define the curl and divergence operator on the space of L^2 vector fields in the distributional sense, i.e.

$$\begin{aligned} \langle \nabla \times F, \Phi \rangle &= \int_{\Omega} F \cdot \nabla \times \Phi \, dx, \quad \forall \Phi \in C_c^\infty(\Omega), \\ \langle \nabla \cdot F, \phi \rangle &= - \int_{\Omega} F \cdot \nabla \phi \, dx, \quad \forall \phi \in C_c^\infty(\Omega). \end{aligned}$$

They induce the spaces

$$\begin{aligned} H(\text{curl}, \Omega) &= \{F \in L^2(\Omega) : \nabla \times F \in L^2(\Omega)\}, \\ H(\text{div}, \Omega) &= \{F \in L^2(\Omega) : \nabla \cdot F \in L^2(\Omega)\} \end{aligned}$$

with the norms

$$\begin{aligned} \|F\|_{H(\text{curl}, \Omega)} &= \|F\|_{L^2(\Omega)} + \|\nabla \times F\|_{L^2(\Omega)}, \\ \|F\|_{H(\text{div}, \Omega)} &= \|F\|_{L^2(\Omega)} + \|\nabla \cdot F\|_{L^2(\Omega)}. \end{aligned}$$

Through integration by parts and density arguments, we can define the tangential trace $F \times \nu \in H^{-1/2}(\partial\Omega)$ for $F \in H(\text{curl}, \Omega)$ by

$$\langle F \times \nu, \Phi \rangle_{\partial\Omega} = \int_{\Omega} F \cdot \nabla \times \Phi \, dx - \int_{\Omega} \nabla \times F \cdot \Phi \, dx, \quad \forall \Phi \in H^1(\Omega),$$

and the normal trace $F \cdot \nu \in H^{-1/2}(\partial\Omega)$ for $F \in H(\text{div}, \Omega)$ by

$$\langle F \cdot \nu, \phi \rangle_{\partial\Omega} = \int_{\Omega} F \cdot \nabla \phi \, dx + \int_{\Omega} (\nabla \cdot F) \phi \, dx, \quad \forall \phi \in H^1(\Omega).$$

Using these definitions and the trace theorem (2.9), we know that

$$\|F \times \nu\|_{H^{-1/2}(\partial\Omega)} \leq C(\Omega) \|F\|_{H(\text{curl}, \Omega)} \quad (2.10)$$

$$\|F \cdot \nu\|_{H^{-1/2}(\partial\Omega)} \leq C(\Omega) \|F\|_{H(\text{div}, \Omega)} \quad (2.11)$$

Further details on these spaces of vector fields can be found in [6, 7].

For notational convenience, we denote the admissible set of electrical conductivities by

$$\begin{aligned} \Sigma(\lambda) &= \{\sigma \in L^\infty(\Omega) : \lambda \leq \sigma \leq \lambda^{-1} \text{ in } \Omega\}, \\ \Sigma(\lambda, \Lambda) &= \{\sigma \in \Sigma(\lambda) \cap W^{1,\infty}(\Omega) : \|\sigma\|_{W^{1,\infty}(\Omega)} \leq \Lambda\} \end{aligned}$$

with constants $\lambda \in (0, 1)$ and $\Lambda > 1$.

2.2 Preliminaries on the adjoint problem

Definition 2.1. We say that $w_L \in H^1(\Omega)$ is a weak solution to the problem (2.7), if for any $\phi \in H^1(\Omega)$,

$$\int_{\Omega} \sigma \nabla w_L \cdot \nabla \phi \, dx = \int_{\Omega} \sigma C_L \cdot \nabla \phi \, dx. \quad (2.12)$$

It is obvious by the definition (2.4) that C_L is smooth in Ω once $L \subset \mathbb{R}^3 \setminus \bar{\Omega}$. Hence, when considering the regularity of the solution w_L , only the regularity of the conductivity σ and the domain Ω matter.

Proposition 2.2. Let Ω be a bounded domain in \mathbb{R}^3 . If $\sigma \in \Sigma(\lambda)$, then

1. the problem (2.7) admits a weak solution, and it is unique up to an additive constant and satisfies

$$\|\nabla w_L\|_{L^2(\Omega)} \leq \lambda^{-2} \|C_L\|_{L^2(\Omega)}; \quad (2.13)$$

2. the total current $J_L = \sigma(C_L - \nabla w_L) \in L^2(\Omega)$ and

$$\|J_L\|_{L^2(\Omega)} \leq C(\lambda) \|C_L\|_{L^2(\Omega)}; \quad (2.14)$$

3. if additionally $\sigma \in W^{1,\infty}(\Omega)$, then $J_L \in H(\text{curl}, \Omega)$.

Proof. The existence and uniqueness up to an additive constant is a standard result by the Poincaré inequality

$$\left\| u - \int_{\Omega} u \, dx \right\|_{L^2(\Omega)} \leq C(\Omega) \|\nabla u\|_{L^2(\Omega)}, \quad \forall u \in H^1(\Omega) \quad (2.15)$$

and the Lax–Milgram theorem. Taking $\phi = w_L$ in (2.12) leads to

$$\lambda \|\nabla w_L\|_{L^2(\Omega)}^2 \leq \lambda^{-1} \|C_L\|_{L^2(\Omega)} \|\nabla w_L\|_{L^2(\Omega)},$$

so the gradient estimate (2.13) holds. Therefore, $J_L = \sigma(C_L - \nabla w_L) \in L^2(\Omega)$ and

$$\|J_L\|_{L^2(\Omega)} \leq \lambda^{-1}(\|C_L\|_{L^2(\Omega)} + \|\nabla w_L\|_{L^2(\Omega)}) \leq C(\lambda)\|C_L\|_{L^2(\Omega)}.$$

Finally, if $\sigma \in W^{1,\infty}(\Omega)$, then by direct computation we see that

$$\nabla \times J_L = \nabla \sigma \times (C_L - \nabla w_L) + \sigma \nabla \times C_L \in L^2(\Omega),$$

yielding that $J_L \in H(\text{curl}, \Omega)$. \square

We also need the following lemma [6, Theorem 3.17], showing that a solenoidal vector field F which is tangential on the boundary admits a normal vector potential A .

Assumption 2.3. *Let Ω be a bounded, simply connected domain in \mathbb{R}^3 with a connected boundary of class $C^{0,1}$.*

Lemma 2.4. *Let Ω satisfy Assumption 2.3. Then for any vector field $F \in H(\text{div}, \Omega)$ satisfying*

$$\begin{cases} \nabla \cdot F = 0 & \text{in } \Omega, \\ F \cdot \nu = 0 & \text{on } \partial\Omega, \end{cases} \quad (2.16)$$

there exists a vector field $A \in H(\text{curl}, \Omega)$ satisfying

$$\begin{cases} \nabla \cdot A = 0 & \text{in } \Omega, \\ A \times \nu = 0 & \text{on } \partial\Omega, \end{cases} \quad (2.17)$$

such that $F = \nabla \times A$ in Ω , and

$$\|A\|_{L^2(\Omega)} \leq C(\Omega)\|F\|_{L^2(\Omega)}. \quad (2.18)$$

Since the equation (2.7) means that the total current J_L satisfies the equation (2.16), we have

Corollary 2.5. *Under Assumption 2.3, if $\sigma \in \Sigma(\lambda)$, then the total current J_L of the problem (2.7) admits a vector potential $A \in H(\text{curl}, \Omega)$, satisfying (2.17) and*

$$\|A\|_{L^2(\Omega)} \leq C(\lambda, \Omega)\|C_L\|_{L^2(\Omega)}. \quad (2.19)$$

3 Inversion procedure

3.1 Recovering the total effect of an acoustic source

In the first step of reconstruction, we consider recovering some information inside Ω from the measured data (2.8). To this end, we proceed as in MAET with voltage measurements [31] to employ the spherical wave

$$p(x, t; y) = \frac{\delta(|x - y| - ct)}{4\pi c^2 t}$$

transmitted at a point y outside the object, which is generated by the initial state

$$p(x, 0; y) = 0, \quad \partial_t p(x, 0; y) = \delta(x - y),$$

so that we can express the measured data as a convolution in space

$$\begin{aligned} m_L(t; y) &= \frac{B_0}{\rho} \cdot \int_{\Omega} J_L(x) \times \nabla_x p(x, t; y) dx \\ &= \left\langle \frac{B_0}{\rho} \cdot (J_L \times \nu \delta_{\partial\Omega} + \nabla \times J_L), p(\cdot, t; y) \right\rangle \\ &= \frac{t}{4\pi} \int_{|z|=1} f(y + ctz) dS_z, \end{aligned}$$

where $f = \frac{B_0}{\rho} \cdot (J_L \times \nu \delta_{\partial\Omega} + \nabla \times J_L)$ is a spatial distribution with support $\bar{\Omega}$, defined by

$$\langle f, \phi \rangle = \frac{B_0}{\rho} \cdot \int_{\Omega} J_L(x) \times \nabla \phi(x) dx, \quad \forall \phi \in C^\infty(\mathbb{R}^3).$$

Hence, the measurement as a function of $t > 0$ and $y \in \mathbb{R}^3 \setminus \bar{\Omega}$, satisfies an acoustic wave equation

$$\begin{cases} (\partial_t^2 - c^2 \Delta_y) m_L(t; y) = 0, & y \in \mathbb{R}^3, t > 0, \\ m_L(0; y) = 0, & y \in \mathbb{R}^3, \\ \partial_t m_L(0; y) = f(y), & y \in \mathbb{R}^3. \end{cases} \quad (3.1)$$

So far we have decoupled the original coupled-physics inverse problem into two parts: an acoustic part and an electromagnetic part. The acoustic part involves an inverse source problem of the acoustic wave equation, to recover the initial state $f(y)$ (which can be regarded as an instantaneous source at the initial time), which is a spatial distribution supported on $\bar{\Omega}$. It also acts as the first inversion step of many other coupled-physics imaging techniques, such as thermo-acoustic tomography (TAT) [11, 22, 30, 39], photo-acoustic tomography (PAT) [12, 27], magneto-acoustic tomography with magnetic induction (MAT-MI) [5, 36], as well as MAET with voltage measurements [31].

When the sound speed is a known constant, as we assume, this inverse source problem is equivalent to the inversion of the spherical mean Radon transform, and has been intensively studied in the literature. Andersson [8] shows that the source f can be inverted from measurements on a plane outside $\bar{\Omega}$ with a Lipschitz stability, using an explicit formula in terms of Fourier transform. An iterative formula is derived in [9]. More studies consider measurements on a closed surface Σ surrounding $\bar{\Omega}$. Explicit inversion formulas are given in [14, 28, 29] for spherical Σ , and in [2, 20] for more general convex Σ . A theoretically exact reconstruction from time-reduced measurements on a finite open surface is also developed in [12]. By the way, when the sound speed $c = c(x)$ varies spatially, the inverse source problem is also studied in [27, 39]. Furthermore, if $c(x)$ is unknown, the joint recovery of $c(x)$ and the initial source f is investigated in [25, 26, 35], where some uniqueness and stability results are derived for specifically structured $c(x)$.

In summary, with sufficiently many measurements generated by external point sources, we are able to determine the spatial distribution f in effective ways mentioned above. Assuming that the mass density ρ of the object is known, the vector-valued distribution $\nabla \times J_L + J_L \times \nu \delta_{\partial\Omega}$ can be determined by setting the background magnetic field B_0 in three axial directions (actually, two directions are sufficient for the determination [31]). After that, the recovered distribution will be used in the electromagnetic part to reconstruct the conductivity σ encoded in the vector field $J_L = \sigma(C_L - \nabla w_L)$.

3.2 Recovering the adjoint current

The information recovered in the first step includes the internal curl and the boundary tangential trace of the adjoint current field $J_L = \sigma(C_L - \nabla w_L)$. Since it satisfies the equation (2.16), we have the following explicit formula for recovering J_L itself:

$$J_L(x) = \nabla \times \int_{\Omega} \nabla_x \times \frac{J_L(y)}{4\pi|x-y|} dy = \nabla \times \left\langle J_L \times \nu \delta_{\partial\Omega} + \nabla \times J_L, \frac{1}{4\pi|x-\cdot|} \right\rangle. \quad (3.2)$$

This formula is given in [40], but for completeness we provide its proof here.

Proof of (3.2). Since $\frac{1}{4\pi|x|}$ is the fundamental solution of $-\Delta$ in \mathbb{R}^3 , we have

$$\begin{aligned} J_L(x) &= \int_{\Omega} J_L(y) \delta(x-y) dy = - \int_{\Omega} \Delta_x \frac{J_L(y)}{4\pi|x-y|} dy \\ &= \nabla \times \int_{\Omega} \nabla_x \times \frac{J_L(y)}{4\pi|x-y|} dy - \nabla \int_{\Omega} \nabla_x \cdot \frac{J_L(y)}{4\pi|x-y|} dy. \end{aligned}$$

The second term vanishes since J_L satisfies the equation (2.16), so that

$$\begin{aligned} \int_{\Omega} \nabla_x \cdot \frac{J_L(y)}{4\pi|x-y|} dy &= \int_{\Omega} J_L(y) \cdot \nabla_x \frac{1}{4\pi|x-y|} dy \\ &= - \int_{\Omega} J_L(y) \cdot \nabla_y \frac{1}{4\pi|x-y|} dy \\ &= - \int_{\partial\Omega} \frac{J_L(y) \cdot \nu(y)}{4\pi|x-y|} dS_y + \int_{\Omega} \frac{\nabla \cdot J_L(y)}{4\pi|x-y|} dy = 0. \end{aligned}$$

Hence, (3.2) is proved. \square

3.3 Recovering the conductivity

Finally, we consider recovering the conductivity σ from the adjoint current $J_L = \sigma(C_L - \nabla w_L)$ in Ω . To this end, we eliminate the gradient to derive

$$\nabla \times \frac{J_L}{\sigma} = \nabla \times C_L = -\frac{\mu}{4\pi} \left[\nabla \left(\nabla \cdot \int_D \frac{n(y)}{|y-x|} dS_y \right) - \Delta \int_D \frac{n(y)}{|y-x|} dS_y \right] \quad (3.3)$$

for $x \in \Omega$. Since $\frac{1}{4\pi|x|}$ is the fundamental solution of $-\Delta$ in \mathbb{R}^3 , we know that

$$-\Delta \int_D \frac{n(y)}{4\pi|y-x|} dS_y = 0$$

provided that D lies outside Ω . Thus the equation (3.3) is equivalent to

$$\nabla \times (rJ_L) = G_L \text{ in } \Omega \quad (3.4)$$

with $r := 1/\sigma$ representing the electrical resistivity and

$$G_L(x) := -\frac{\mu}{4\pi} \nabla \left(\nabla \cdot \int_D \frac{n(y)}{|y-x|} dS_y \right) = -\frac{\mu}{4\pi} \int_D \left(3 \frac{(y-x) \cdot n(y)}{|y-x|^5} (y-x) - \frac{n(y)}{|y-x|^3} \right) dS_y$$

depending only on the coil L . Noting that (3.4) constitutes an overdetermined system of linear partial differential equations for r , it can be recast as the least-squares problem

$$\min_r \frac{1}{2} \|\nabla \times (rJ_L) - G_L\|_{L^2(\Omega)}^2,$$

which can be solved using standard gradient-based iterative methods.

In conclusion, we have designed an inversion procedure to reconstruct the conductivity distribution, which is shown in Figure 2.

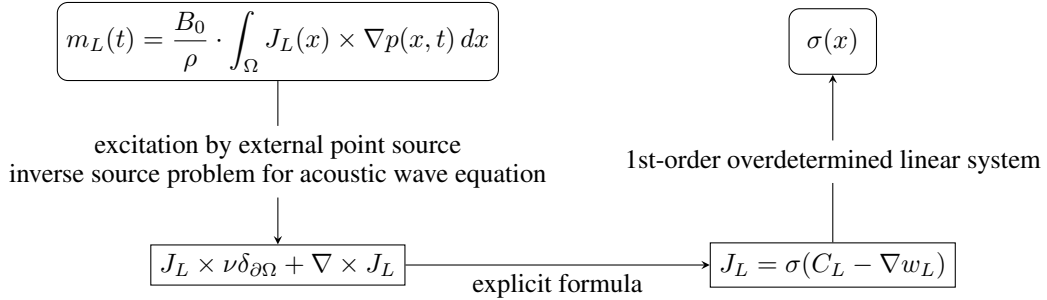


Figure 2: Diagram of inversion procedure

4 Stability of recovering the conductivity from an internal current density

Within the inversion framework described above, the acoustic inverse source problem has been extensively investigated in the literature, and a variety of efficient reconstruction methods are available. Consequently, the remaining task is to analyze the stability of recovering the conductivity σ from the measured current density field J_L .

The well-posedness of the forward problem has been established in Proposition 2.2. More precisely, for any fixed coil L located outside the domain Ω , the forward operator

$$\mathcal{F}_L: \Sigma(\lambda, \Lambda) \rightarrow H(\text{curl}, \Omega), \quad \sigma \mapsto J_L = \sigma(C_L - \nabla w_L) \quad (4.1)$$

is well-defined. In what follows, we fix a coil L and investigate the stability of reconstructing σ from the data $\mathcal{F}_L(\sigma)$.

Proposition 4.1. *Let Ω satisfy Assumption 2.3 and $\sigma_1, \sigma_2 \in \Sigma(\lambda, \Lambda)$. If $J_1 = \mathcal{F}_L(\sigma_1)$ and $J_2 = \mathcal{F}_L(\sigma_2)$, then*

$$\int_{\Omega} |\sigma_1 - \sigma_2| |J_1|^2 dx \leq C(\lambda, \Lambda, \Omega) \|C_L\|_{L^2(\Omega)} \|J_1 - J_2\|_{H(\text{curl}, \Omega)}. \quad (4.2)$$

Proof. Let $r_1 = 1/\sigma_1$ and $r_2 = 1/\sigma_2$. Then

$$\nabla \times (r_1 J_1) = G_L = \nabla \times (r_2 J_2) \text{ in } \Omega.$$

It follows that

$$\nabla \times [(r_1 - r_2)J_1] = \nabla \times [r_2(J_2 - J_1)] \text{ in } \Omega.$$

Let sgn be the sign function on \mathbb{R} , that is,

$$\text{sgn}(t) = \begin{cases} 1, & t > 0, \\ 0, & t = 0, \\ -1, & t < 0. \end{cases}$$

Then

$$\begin{aligned} \nabla \times (|r_1 - r_2|J_1) &= \nabla|r_1 - r_2| \times J_1 + |r_1 - r_2|\nabla \times J_1 \\ &= \text{sgn}(r_1 - r_2)[\nabla(r_1 - r_2) \times J_1 + \nabla \times J_1] \\ &= \text{sgn}(r_1 - r_2)\nabla \times [(r_1 - r_2)J_1] \\ &= \text{sgn}(r_1 - r_2)\nabla \times [r_2(J_2 - J_1)]. \end{aligned} \quad (4.3)$$

By [Corollary 2.5](#), there exists a vector field $A \in H^1(\Omega)$ satisfying [\(2.17\)](#) and [\(2.19\)](#) such that $J_1 = \nabla \times A$. Multiplying both sides of the equality [\(4.3\)](#) by A and integrating the left-hand side by parts, we have

$$\int_{\Omega} |r_1 - r_2||J_1|^2 dx = \int_{\Omega} \text{sgn}(r_1 - r_2)A \cdot \nabla \times [r_2(J_2 - J_1)] dx,$$

where the boundary term vanishes since $A \times \nu = 0$ on $\partial\Omega$. It follows that

$$\begin{aligned} \int_{\Omega} |r_1 - r_2||J_1|^2 dx &\leq \|A\|_{L^2(\Omega)} \|r_2\|_{W^{1,\infty}(\Omega)} \|J_1 - J_2\|_{H(\text{curl},\Omega)} \\ &\leq C(\lambda, \Lambda, \Omega) \|C_L\|_{L^2(\Omega)} \|J_1 - J_2\|_{H(\text{curl},\Omega)}. \end{aligned}$$

Noting that

$$|r_1 - r_2| = \frac{|\sigma_1 - \sigma_2|}{\sigma_1 \sigma_2} \geq \lambda^2 |\sigma_1 - \sigma_2|,$$

the weighted estimate [\(4.2\)](#) is proved. \square

Remark 4.2. We emphasize that no boundary condition of the form $\sigma_1 = \sigma_2$ on $\partial\Omega$ is required. Indeed, one can select a vector potential A associated with J_1 such that $A \times \nu = 0$ on $\partial\Omega$, which eliminates the boundary contribution arising from integration by parts. This observation highlights a structural advantage of the magnetic field measurement mode in MAET: the internal conductivity can, in principle, be stably recovered without any a priori knowledge of its boundary values.

This weighted estimate shows that r can be uniquely determined where $J_1 \neq 0$, and can be stably recovered where $|J_1|$ admits a positive lower bound.

Example 4.3. If D is in a plane P outside Ω , then its normal vector n is constant. Suppose $P = \{y \in \mathbb{R}^3 : y \cdot n = a\}$ with $a \in \mathbb{R}$. Then

$$C_L(x) = -\frac{\mu}{4\pi} \int_D \frac{y-x}{|y-x|^3} dS_y \times n, \quad (4.4)$$

$$\begin{aligned} G_L(x) &= -\frac{\mu}{4\pi} \left[\int_D \frac{3(y-x) \cdot n}{|y-x|^5} (y-x) dS_y - \left(\int_D \frac{1}{|y-x|^3} dS_y \right) n \right] \\ &= -\frac{\mu}{4\pi} \left[3(a-x \cdot n) \int_D \frac{y-x}{|y-x|^5} dS_y - \left(\int_D \frac{1}{|y-x|^3} dS_y \right) n \right]. \end{aligned} \quad (4.5)$$

Here, note that $|a - x \cdot n| = \text{dist}(x, P)$.

Furthermore, if D is a disk, say $D = B(y_0, r) \cap P$ with $r > 0$ and $y_0 \in P$:

- for $x \in y_0 + \mathbb{R}n$, which is the central axis of D : by symmetry we have

$$\int_D \frac{y-x}{|y-x|^5} dS_y = (a-x \cdot n) \left(\int_D \frac{1}{|y-x|^5} dS_y \right) n,$$

so

$$G_L(x) = -\frac{\mu}{4\pi} \left[3 \operatorname{dist}(x, P)^2 \int_D \frac{1}{|y-x|^5} dS_y - \int_D \frac{1}{|y-x|^3} dS_y \right] n,$$

which is nonzero if

$$\operatorname{dist}(x, P) > \frac{1}{\sqrt{3}} \sup_{y \in D} |y-x|.$$

In particular, $G_L \neq 0$ everywhere in $\Omega \cap (y_0 + \mathbb{R}n)$ provided that $\operatorname{dist}(\Omega, P) > \operatorname{diam}(\Omega \cup D)/\sqrt{3}$;

- for $x \notin y_0 + \mathbb{R}n$: since D has a symmetry plane across x , the integral

$$\int_D \frac{y-x}{|y-x|^3} dS_y$$

must point to a direction that is not parallel to n , so $G_L(x) \neq 0$ noting that $|a-x \cdot n| = \operatorname{dist}(x, P) > 0$.

It shows that J_L cannot vanish identically in any open subset of Ω , otherwise it contradicts the equation (3.4). This non-vanishing property of J_L provides encouraging evidence for our expectation that $|J_L|$ is bounded away from zero.

4.1 Nonzero constraint and stability in bounded domain

One approach to guarantee that J_L is nonzero in a subdomain Ω' is to derive the estimate

$$0 < \sup_{\Omega'} |\nabla w_L| \leq \frac{1}{2} \inf_{\Omega'} |C_L|.$$

In this way, we need to assume

Assumption 4.4. *There exists a constant $c > 0$ and a subdomain Ω' of Ω , such that $|C_L| \geq c$ in Ω' .*

Theorem 4.5. *Let Ω satisfy Assumption 2.3 with $\partial\Omega \in C^{1,\alpha}$ for an $\alpha \in (0, 1)$ and $q = \frac{3}{1-\alpha}$. If $\sigma \in \Sigma(\lambda, \Lambda)$ and Assumption 4.4 holds, then there exists a constant C_1 depending on λ, Λ, α and Ω , such that if*

$$\|\nabla \cdot (\sigma C_L)\|_{L^q(\Omega)} + \|C_L \cdot \nu\|_{C^{0,\alpha}(\partial\Omega)} \leq \frac{c}{2C_1}, \quad (4.6)$$

then $J_L = \sigma(C_L - \nabla w_L)$ with w_L solving (2.7) satisfies

$$|J_L| \geq \frac{\lambda c}{2} \text{ in } \Omega'.$$

Proof. Without loss of generality, we assume that $\int_{\Omega} w_L dx = 0$, since by Proposition 2.2, the solution w_L is unique up to an additive constant. Then by Poincaré's inequality (2.15) and testing the equation (2.7) with w_L itself we have

$$\|w_L\|_{L^2(\Omega)} \leq C(\Omega) \|\nabla w_L\|_{L^2(\Omega)} \leq C(\lambda, \Omega) \left(\|\nabla \cdot (\sigma C_L)\|_{L^2(\Omega)} + \|C_L \cdot \nu\|_{L^2(\partial\Omega)} \right).$$

Combining Theorem 5.31 and Corollary 5.32 in [34], we derive

$$\begin{aligned} \|w_L\|_{L^\infty(\Omega)} &\leq C(\lambda, \alpha, \Omega) \left(\|w_L\|_{L^2(\Omega)} + \|\nabla \cdot (\sigma C_L)\|_{L^q(\Omega)} + \|C_L \cdot \nu\|_{L^\infty(\partial\Omega)} \right) \\ &\leq C(\lambda, \alpha, \Omega) \left(\|\nabla \cdot (\sigma C_L)\|_{L^q(\Omega)} + \|C_L \cdot \nu\|_{L^\infty(\partial\Omega)} \right). \end{aligned}$$

By the Schauder estimate [34, Theorem 5.54]

$$\|w_L\|_{C^{1,\alpha}(\bar{\Omega})} \leq C(\lambda, \Lambda, \Omega) \left(\|w_L\|_{L^\infty(\Omega)} + \|\nabla \cdot (\sigma C_L)\|_{L^q(\Omega)} + \|C_L \cdot \nu\|_{C^{0,\alpha}(\partial\Omega)} \right).$$

we have

$$\|\nabla w_L\|_{L^\infty(\Omega)} \leq C_1(\lambda, \Lambda, \alpha, \Omega) \left(\|\nabla \cdot (\sigma C_L)\|_{L^q(\Omega)} + \|C_L \cdot \nu\|_{C^{0,\alpha}(\partial\Omega)} \right).$$

Therefore, if (4.6) holds with the constant C_1 above, we have

$$\|\nabla w_L\|_{L^\infty(\Omega)} \leq \frac{c}{2},$$

so that

$$|J_L| \geq \lambda |C_L - \nabla w_L| \geq \frac{\lambda c}{2} \text{ in } \Omega'.$$

□

Remark 4.6. *The smallness condition (4.6) actually contains two requirements:*

1. *Since $\nabla \cdot C_L = 0$, we have $\nabla \cdot (\sigma C_L) = \nabla \sigma \cdot C_L$, so the bound requires that C_L should be “almost orthogonal” to the deviation of σ . For example, if σ varies only in one direction e , then we can set the coil L in a plane with normal e , so that $\nabla \sigma \cdot C_L = 0$ since $C_L \perp e$.*
2. *The second part requires that C_L is “almost tangential” on $\partial\Omega$. For example, if Ω is rotationally symmetric with an axis $\mathbb{R}e$, then we can set the coil L as a circle with the same axis, so that $C_L \cdot \nu = 0$ on $\partial\Omega$ since C_L circulates around this axis; see Figure 3. However, such C_L vanishes on the axis, so we can only guarantee the non-vanishing property of J_L in Ω' that is away from the axis.*

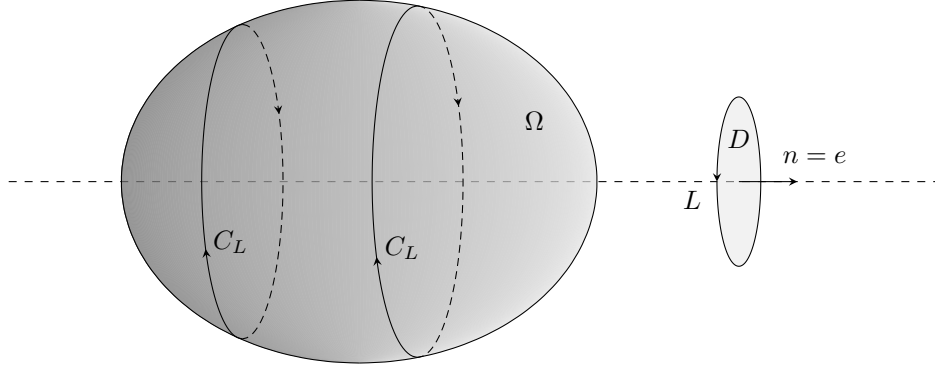


Figure 3: Rotationally symmetric domain and coil with the same axis

Through the weighted estimate (4.2), we directly obtain the following conditional stability result.

Corollary 4.7. *Let Ω satisfy Assumption 2.3 with $\partial\Omega \in C^{1,\alpha}$ for an $\alpha \in (0, 1)$ and $q = \frac{3}{1-\alpha}$. Suppose Assumption 4.4 holds. If $\sigma_1, \sigma_2 \in \Sigma(\lambda, \Lambda)$, then there exists a constant C_1 depending on $\lambda, \Lambda, \alpha, \Omega$ such that if*

$$\|\nabla \sigma_1 \cdot C_L\|_{L^q(\Omega)} + \|C_L \cdot \nu\|_{C^{0,\alpha}(\partial\Omega)} \leq \frac{c}{2C_1},$$

then

$$\|\sigma_1 - \sigma_2\|_{L^1(\Omega')} \leq C_S \|C_L\|_{L^2(\Omega)} \|\mathcal{F}_L(\sigma_1) - \mathcal{F}_L(\sigma_2)\|_{H(\text{curl}, \Omega)} \quad (4.7)$$

for some constant $C_S > 0$ depending on $\lambda, \Lambda, \alpha, \Omega$ and c .

4.2 Nonzero constraint and stability in half-space

Now we consider when the imaging domain Ω is regarded as a half-space, say $\mathbb{R}_+^3 := \mathbb{R}^2 \times (0, \infty)$, which is a reasonable approximation of the scenario that the coil L is placed near a flat surface of a biological tissue. Setting L in a plane parallel to $\partial\Omega = \mathbb{R}^2 \times \{0\}$, we know from (4.4) that $C_L \cdot \nu = 0$ on $\partial\Omega$, so that the smallness condition (4.6) contains only the source term.

However, we cannot directly use the estimates above to derive analogous results, since Ω is unbounded in this case. For simplicity, we make the following assumptions; see Figure 4.

Assumption 4.8. *Let $\sigma: \mathbb{R}_+^3 \rightarrow \mathbb{R}_+$ satisfy*

- $\sigma \equiv \sigma_0$ outside a half-ball $B_+(R) := \mathbb{R}_+^3 \cap \{|x| < R\}$ with $R \geq 1$;
- $\sigma \in \Sigma(\lambda, \Lambda)$ with Ω replaced by $B_+(R)$.

Noting that $\sigma \in C^0(\overline{B_+(R)})$ by Sobolev embedding, we further assume that

- σ is continuous across the interface $\partial B_+(R) \cap \mathbb{R}_+^3$.

With this assumption, the solution of (2.7) can be expressed using a Green function of the operator $-\nabla \cdot (\sigma \nabla)$ with Neumann boundary condition in the half-space \mathbb{R}_+^3 :

$$w_L(x) = - \int_{B_+(R)} G(x, y) f(y) dy \quad (4.8)$$

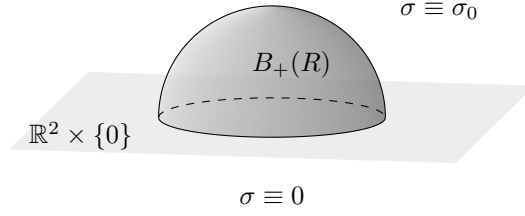


Figure 4: Assumptions of conductivity distribution in half-space

with $f = \nabla \sigma \cdot C_L$, which vanishes outside $B_+(R)$ due to the first assumption on σ . The existence of G and its well-known global pointwise estimate

$$0 \leq G(x, y) \leq C(\lambda)|x - y|^{-1}, \quad x \neq y, \quad (4.9)$$

can be demonstrated as in [21] and [24] for Dirichlet problem in unbounded domain. Using the Green function representation (4.8) and the pointwise estimate (4.9), we first derive that for any $x \in B_+(2R)$,

$$\begin{aligned} |w_L(x)| &\leq C(\lambda) \int_{B_+(R)} \frac{|f(y)|}{|x - y|} dy \\ &\leq C(\lambda) \|f\|_{L^\infty(B_+(R))} R^2. \end{aligned} \quad (4.10)$$

Next, we proceed as in [17, Lemma 3.1] to derive the pointwise estimate of ∇w_L in $B_+(R)$:

Lemma 4.9. *Let $\sigma \in \Sigma(\lambda, \Lambda)$ with Ω replaced by \mathbb{R}_+^3 . Suppose v is a bounded solution to*

$$\begin{cases} \nabla \cdot (\sigma \nabla v) = f & \text{in } \mathbb{R}_+^3, \\ \partial_\nu v = 0 & \text{on } \partial \mathbb{R}_+^3 \end{cases}$$

with $f \in L^\infty(\mathbb{R}_+^3)$. Then for any $R > 0$,

$$\|\nabla v\|_{L^\infty(B_+(R))} \leq C(\lambda, \Lambda) \left(R \|f\|_{L^\infty(B_+(2R))} + \frac{1}{R} \|v\|_{L^\infty(B_+(2R))} \right). \quad (4.11)$$

Proof. By a scaling argument, we only need to prove the result for $R = 1$. First of all, it follows from the regularity assumptions that $v \in C^1(\overline{B_+(1)})$. Denote

$$M_0 := \|v\|_{L^\infty(B_+(2))}, \quad M_1 := \|\nabla v\|_{L^\infty(B_+(1))}$$

and let $M_1 = |\nabla v(x_0)|$ for some $x_0 \in \overline{B_+(1)}$. For any $r \leq 1/2$, define a cut-off function $\eta \in C_c^\infty(B(x_0, r))$ satisfying

$$0 \leq \eta \leq 1, \quad \eta = 1 \text{ in } B(x_0, r/2), \quad |\nabla \eta| \leq \frac{C}{r}, \quad |\Delta \eta| \leq \frac{C}{r^2}.$$

Let

$$G_0(x, y) = \frac{1}{4\pi\sigma(x_0)} \left(\frac{1}{|x - y|} - \frac{1}{|x - \tilde{y}|} \right), \quad x, y \in \mathbb{R}_+^3$$

with $\tilde{y} = (y_1, y_2, -y_3)$ be the Green solution of the operator $-\sigma(x_0)\Delta$ with Dirichlet boundary condition in \mathbb{R}_+^3 . Since v satisfies the homogeneous Neumann boundary condition on the flat boundary $\partial \mathbb{R}_+^3$, we can use $\eta G_0(\cdot, y)$ with arbitrary $y \in B_r := \mathbb{R}_+^3 \cap B(x_0, r)$ as a test function, leading to

$$\begin{aligned} - \int_{B_r} f \eta G_0 dx &= \int_{B_r} \sigma \nabla v \cdot \nabla_x (\eta G_0) dx \\ &= \sigma(x_0) \int_{B_r} \nabla v \cdot (\eta \nabla_x G_0 + G_0 \nabla \eta) dx \\ &\quad + \int_{B_r} (\sigma - \sigma(x_0)) \nabla v \cdot (\eta \nabla_x G_0 + G_0 \nabla \eta) dx. \end{aligned} \quad (4.12)$$

Due to the choice of η and G_0 , integrating the first term by parts, it becomes

$$\begin{aligned} & \sigma(x_0) \int_{B_r} \nabla v \cdot (\eta \nabla_x G_0 + G_0 \nabla \eta) dx \\ &= \sigma(x_0) \int_{B_r} [\nabla(\eta v) - v \nabla \eta] \cdot \nabla_x G_0 dx - \sigma(x_0) \int_{B_r} v \nabla_x \cdot (G_0 \nabla \eta) dx \\ &= \eta(y)v(y) - \sigma(x_0) \int_{B_r} v(2\nabla \eta \cdot \nabla_x G_0 + G_0 \Delta \eta) dx. \end{aligned}$$

Therefore, for $i = 1, 2, 3$, differentiating (4.12) with respect to y_i and letting $y = x_0$ we obtain

$$\begin{aligned} \partial_i v(x_0) &= - \int_{B_r} f \eta \partial_{y_i} G_0(x, x_0) dx \\ &+ \sigma(x_0) \int_{B_r} v[2\nabla \eta \cdot \partial_{y_i} \nabla_x G_0(x, x_0) + \Delta \eta \partial_{y_i} G_0(x, x_0)] dx \\ &+ \int_{B_r} (\sigma - \sigma(x_0)) \nabla v \cdot [\eta \partial_{y_i} \nabla_x G_0(x, x_0) + \partial_{y_i} G_0(x, x_0) \nabla \eta] dx. \end{aligned}$$

Since direct computations on G_0 show that

$$|\nabla_y G_0(x, y)| \leq C(\lambda) |x - y|^{-2}, \quad |\nabla_y \nabla_x G_0(x, y)| \leq C(\lambda) |x - y|^{-3}$$

for all $x, y \in \mathbb{R}_+^3$, we derive that

$$\begin{aligned} M_1 = |\nabla v(x_0)| &\leq C(\lambda) \left(\int_{B_r} \frac{|f(x)|}{|x - x_0|^2} dx + \frac{M_0}{r} \int_{B_r \setminus B_{r/2}} \frac{1}{|x - x_0|^3} dx + \frac{M_0}{r^2} \int_{B_r \setminus B_{r/2}} \frac{1}{|x - x_0|^2} dx \right) \\ &+ C(\lambda, \Lambda) M_1 \left(\int_{B_r} \frac{1}{|x - x_0|^2} dx + \frac{1}{r} \int_{B_r \setminus B_{r/2}} \frac{1}{|x - x_0|} dx \right) \\ &\leq C(\lambda) \left(\|f\|_{L^\infty(B_+(2))} r + \frac{M_0}{r} \right) + C_0(\lambda, \Lambda) M_1 r. \end{aligned}$$

Taking $r = \min(\frac{1}{2}, \frac{1}{2C_0})$ yields that

$$M_1 \leq C(\lambda, \Lambda) \left(\|f\|_{L^\infty(B_+(2))} + M_0 \right),$$

which is (4.11) with $R = 1$. □

Combining (4.11) with the estimate (4.10), we obtain

$$\sup_{B_+(R)} |\nabla w_L| \leq C_1(\lambda, \Lambda) R \|\nabla \sigma \cdot C_L\|_{L^\infty(B_+(R))}. \quad (4.13)$$

In conclusion, we have

Theorem 4.10. *Let σ_1, σ_2 satisfy Assumption 4.8 and $J_1 = \mathcal{F}_L(\sigma_1)$, $J_2 = \mathcal{F}_L(\sigma_2)$. Suppose*

- $L \subset \mathbb{R}^2 \times \{-a\}$ with $a > 0$, and
- $|C_L| \geq c$ for a constant $c > 0$ in a subdomain Ω' of $B_+(R)$.

Then there exists a constant C_1 depending on λ, Λ , such that if

$$\|\nabla \sigma_1 \cdot C_L\|_{L^\infty(B_+(R))} \leq \frac{c}{2C_1 R}, \quad (4.14)$$

then $|J_1| \geq \lambda c/2$ in Ω' , and

$$\|\sigma_1 - \sigma_2\|_{L^1(\Omega')} \leq C_S R^{5/2} \|J_1 - J_2\|_{H(\text{curl}, B_+(R))} \quad (4.15)$$

for some constant $C_S > 0$ depending on λ, Λ, a, c and the area bounded by L .

Remark 4.11. *The parameter R is the radius of the region within which the conductivity σ is inhomogeneous and the source $\nabla\sigma \cdot C_L$ is supported. It impacts the stability estimate in two ways: a larger R results in a more restrictive smallness condition (4.14) on the unknown conductivity, as well as a larger stability constant $C_S R^{5/2}$.*

The lower bound of $|J_1|$ comes directly from (4.13) and (4.14). To derive the stability estimate (4.15), we still cannot directly use the previous weighted estimate (4.2), since it involves the application of Lemma 2.4. This result of normal vector potential only applies for bounded domains and for vector fields that are tangential on the whole boundary. Now if we tend to find a vector potential A of J_1 in $B_+(R)$, since J_1 is tangential only on the flat boundary $\Gamma_0 := \partial B_+(R) \cap \partial \mathbb{R}_+^3$, we can only construct A that is normal on Γ_0 . The idea is to extend J_1 to a slightly larger half-ball so that it is tangential on the whole boundary, and we can apply Lemma 2.4.

Lemma 4.12. *For any vector field $F \in H(\operatorname{div}, B_+(R))$ satisfying*

$$\begin{cases} \nabla \cdot F = 0 & \text{in } B_+(R), \\ F \cdot \nu = 0 & \text{on } \Gamma_0, \end{cases} \quad (4.16)$$

there exists a vector field $A \in H(\operatorname{curl}, B_+(R))$ satisfying

$$\begin{cases} \nabla \cdot A = 0 & \text{in } B_+(R), \\ A \times \nu = 0 & \text{on } \Gamma_0 \end{cases} \quad (4.17)$$

and a generic constant $C > 0$, such that $F = \nabla \times A$ in $B_+(R)$ and

$$\|A\|_{L^2(B_+(R))} \leq CR \|F\|_{L^2(B_+(R))}. \quad (4.18)$$

Proof. By a scaling argument, we only need to prove this result for $R = 1$. Denote

$$D := B_+(2) \setminus \overline{B_+(1)}, \quad \Gamma := \partial B_+(1) \cap \mathbb{R}_+^3.$$

Let $\psi \in H^1(D)$ be a weak solution of the Neumann problem

$$\begin{cases} \Delta \psi = 0 & \text{in } D, \\ \partial_\nu \psi = F \cdot \nu & \text{on } \Gamma, \\ \partial_\nu \psi = 0 & \text{on } \partial D \setminus \Gamma. \end{cases}$$

It is unique up to an additive constant, so we take the one satisfying $\int_D \psi \, dx = 0$. Then by the trace theorem (2.9) and Poincaré's inequality (2.15), we have

$$\|\nabla \psi\|_{L^2(D)}^2 = \langle F \cdot \nu, \psi \rangle_\Gamma \leq \|\psi\|_{H^{1/2}(\Gamma)} \|F \cdot \nu\|_{H^{-1/2}(\Gamma)} \leq C \|\nabla \psi\|_{L^2(D)} \|F \cdot \nu\|_{H^{-1/2}(\Gamma)}.$$

Therefore,

$$\|\nabla \psi\|_{L^2(D)} \leq C \|F \cdot \nu\|_{H^{-1/2}(\Gamma)} \leq C \|F\|_{L^2(B_+(1))},$$

where the last inequality is due to the estimate (2.11) of the normal trace and the fact that F is solenoidal in $B_+(1)$. Now let

$$\tilde{F} = \begin{cases} F & \text{in } B_+(1), \\ \nabla \psi & \text{in } D. \end{cases}$$

Since $\tilde{F} \in L^2(B_+(2))$ satisfying

$$\begin{cases} \nabla \cdot \tilde{F} = 0 & \text{in } B_+(2), \\ \tilde{F} \cdot \nu = 0 & \text{on } \partial B_+(2), \end{cases}$$

by Lemma 2.4 it admits a vector potential $\tilde{A} \in H(\operatorname{curl}, B_+(2))$ satisfying

$$\begin{cases} \nabla \cdot \tilde{A} = 0 & \text{in } B_+(2), \\ \tilde{A} \times \nu = 0 & \text{on } \partial B_+(2) \end{cases}$$

and

$$\|\tilde{A}\|_{L^2(B_+(2))} \leq C \|\tilde{F}\|_{L^2(B_+(2))} \leq C \|F\|_{L^2(B_+(1))}.$$

Then $A := \tilde{A}|_{B_+(1)}$ is a vector potential of F and satisfies (4.17) and (4.18) with $R = 1$. \square

Proof of Theorem 4.10. It remains to prove (4.15). Analogously to the proof of Proposition 4.1, by applying Lemma 4.12 to J_1 instead of using Corollary 2.5 we have

$$\begin{aligned} \int_{B_+(R)} |\sigma_1 - \sigma_2| |J_1|^2 dx &\leq C(\lambda, \Lambda) \|A\|_{L^2(B_+(R))} \|J_1 - J_2\|_{H(\text{curl}, B_+(R))} \\ &\leq C(\lambda, \Lambda) R \|J_1\|_{L^2(B_+(R))} \|J_1 - J_2\|_{H(\text{curl}, B_+(R))}. \end{aligned} \quad (4.19)$$

Now we estimate the L^2 norm of J_1 . By Caccioppoli's inequality, the weak solution w_1 of (2.7) with $\sigma = \sigma_1$ satisfies the estimate

$$\|\nabla w_1\|_{L^2(B_+(R))} \leq C(\lambda) \left(R \|\nabla \sigma_1 \cdot C_L\|_{L^2(B_+(R))} + \frac{1}{R} \|w_1\|_{L^2(B_+(2R))} \right).$$

Using the Green function representation (4.8) and the pointwise estimate (4.9) we derive

$$\|w_1\|_{L^2(B_+(2R))} \leq C(\lambda) R^2 \|\nabla \sigma_1 \cdot C_L\|_{L^2(B_+(R))}.$$

So

$$\|\nabla w_1\|_{L^2(B_+(R))} \leq C(\lambda) R \|\nabla \sigma_1 \cdot C_L\|_{L^2(B_+(R))}$$

and by the smallness condition (4.14), we have

$$\|\nabla w_1\|_{L^2(B_+(R))} \leq C(\lambda, \Lambda, c) R^{3/2}.$$

Moreover, according to (2.4), we know that $|C_L| \leq C a^{-2} \text{Area } D$, leading to the estimate

$$\|C_L\|_{L^2(B_+(R))} \leq C(a, \text{Area } D) R^{3/2}.$$

Thus,

$$\|J_1\|_{L^2(B_+(R))} \leq \lambda^{-1} \left(\|C_L\|_{L^2(B_+(R))} + \|\nabla w_1\|_{L^2(B_+(R))} \right) \leq C(\lambda, \Lambda, a, c, \text{Area } D) R^{3/2}. \quad (4.20)$$

Finally, (4.15) follows from (4.19), (4.20) and the previous result that $|J_1| \geq \lambda c/2$ in $\Omega' \subset B_+(R)$. \square

5 Concluding remarks

In conclusion, this work provides a rigorous mathematical foundation for MAET with magnetic field measurements. We formulate a quasi-static model that accurately captures the underlying physics and introduce an adjoint problem to decouple the hybrid inverse problem. This decoupling yields a well-studied acoustic inverse source problem and a critical inverse conductivity problem with internal data. Our primary theoretical contribution lies in addressing the latter, where a nonzero constraint on the data is required for stable reconstruction. By proposing some smallness conditions on the conductivity and coil configuration, we derive Lipschitz stability results in both bounded domains and half-space. This framework not only justifies existing experimental setups but also provides clear guidelines for optimizing coil design to enhance imaging resolution.

References

- [1] R. A. Adams and J. J. F. Fournier. *Sobolev Spaces*, volume 140 of *Pure and Applied Mathematics*. Academic Press, Oxford, 2nd edition, 2003.
- [2] M. Agranovsky and L. Kunyansky. On the exactness of the universal backprojection formula for the spherical means Radon transform. *Inverse Problems*, 39(3):035002, 2023.
- [3] G. S. Alberti. Non-zero constraints in elliptic PDE with random boundary values and applications to hybrid inverse problems. *Inverse Problems*, 38(12):124005, 2022.
- [4] G. S. Alberti and Y. Capdeboscq. *Lectures on Elliptic Methods for Hybrid Inverse Problems*, volume 25 of *Collection SMF Cours spécialisés*. Société mathématique de France, Paris, 2018.
- [5] H. Ammari, S. Boulmier, and P. Millien. A mathematical and numerical framework for magnetoacoustic tomography with magnetic induction. *Journal of Differential Equations*, 259(10):5379–5405, 2015.
- [6] C. Amrouche, C. Bernardi, M. Dauge, and V. Girault. Vector potentials in three-dimensional non-smooth domains. *Mathematical Methods in the Applied Sciences*, 21(9):823–864, 1998.
- [7] C. Amrouche and N. E. H. Seloula. Lp-theory for vector potentials and Sobolev's inequalities for vector fields: Application to the Stokes equations with pressure boundary conditions. *Mathematical Models and Methods in Applied Sciences*, 23(01):37–92, 2013.

- [8] L.-E. Andersson. On the determination of a function from spherical averages. *SIAM Journal on Mathematical Analysis*, 19(1):214–232, 1988.
- [9] R. Aramyan. Recovering a function from spherical means in 3D using local data. *Inverse Problems and Imaging*, 18(3):690–707, 2024.
- [10] G. Bal. Hybrid inverse problems and internal functionals. In G. Uhlmann, editor, *Inverse Problems and Applications: Inside out II*, volume 60 of *Mathematical Sciences Research Institute Publications*, pages 325–368. Cambridge University Press, Cambridge, 2013.
- [11] G. Bal, K. Ren, G. Uhlmann, and T. Zhou. Quantitative thermo-acoustics and related problems. *Inverse Problems*, 27(5):055007, 2011.
- [12] N. Do and L. Kunyansky. Theoretically exact photoacoustic reconstruction from spatially and temporally reduced data. *Inverse Problems*, 34(9):094004, 2018.
- [13] L. C. Evans. *Partial Differential Equations*, volume 19 of *Graduate Studies in Mathematics*. American Mathematical Society, Providence, Rhode Island, 2nd edition, 2010.
- [14] D. Finch, S. K. Patch, and Rakesh. Determining a function from its mean values over a family of spheres. *SIAM Journal on Mathematical Analysis*, 35(5):1213–1240, 2004.
- [15] N. G. Gençer and M. N. Tek. Electrical conductivity imaging via contactless measurements. *IEEE Transactions on Medical Imaging*, 18(7):617–627, 1999.
- [16] M. S. Gözü and N. G. Gençer. Analyzing pulse compression performance and image quality metrics of different excitations in MAET with magnetic field measurements. *International Journal for Numerical Methods in Biomedical Engineering*, 40(12):e3890, 2024.
- [17] M. Grüter and K.-O. Widman. The Green function for uniformly elliptic equations. *manuscripta mathematica*, 37(3):303–342, 1982.
- [18] L. Guo, G. Liu, and H. Xia. Magneto-acousto-electrical tomography with magnetic induction for conductivity reconstruction. *IEEE Transactions on Biomedical Engineering*, 62(9):2114–2124, 2015.
- [19] S. Haider, A. Hrbek, and Y. Xu. Magneto-acousto-electrical tomography: A potential method for imaging current density and electrical impedance. *Physiological Measurement*, 29(6):S41–S50, 2008.
- [20] M. Haltmeier. Universal inversion formulas for recovering a function from spherical means. *SIAM Journal on Mathematical Analysis*, 46(1):214–232, 2014.
- [21] S. Hofmann and S. Kim. The Green function estimates for strongly elliptic systems of second order. *manuscripta mathematica*, 124(2):139–172, 2007.
- [22] Y. Hristova, P. Kuchment, and L. Nguyen. Reconstruction and time reversal in thermoacoustic tomography in acoustically homogeneous and inhomogeneous media. *Inverse Problems*, 24(5):055006, 2008.
- [23] K. Kaboutari, A. Ö. Tetik, E. Ghalichi, M. S. Gözü, R. Zengin, and N. G. Gençer. Data acquisition system for MAET with magnetic field measurements. *Physics in Medicine & Biology*, 64(11):115016, 2019.
- [24] K. Kang and S. Kim. Global pointwise estimates for Green’s matrix of second order elliptic systems. *Journal of Differential Equations*, 249(11):2643–2662, 2010.
- [25] Y. Kian and H. Liu. Uniqueness and stability in determining the wave equation from a single passive boundary measurement, 2025.
- [26] Y. Kian and G. Uhlmann. Determination of the sound speed and an initial source in photoacoustic tomography. *Transactions of the American Mathematical Society*, 378(8):5329–5353, 2025.
- [27] P. Kuchment and L. Kunyansky. Mathematics of photoacoustic and thermoacoustic tomography. In O. Scherzer, editor, *Handbook of Mathematical Methods in Imaging*, pages 817–865. Springer, New York, 2011.
- [28] L. Kunyansky. Explicit inversion formulae for the spherical mean Radon transform. *Inverse Problems*, 23(1):373–383, 2007.
- [29] L. Kunyansky. A series solution and a fast algorithm for the inversion of the spherical mean Radon transform. *Inverse Problems*, 23(6):S11–S20, 2007.
- [30] L. Kunyansky. Thermoacoustic tomography with detectors on an open curve: An efficient reconstruction algorithm. *Inverse Problems*, 24(5):055021, 2008.
- [31] L. Kunyansky. A mathematical model and inversion procedure for magneto-acousto-electric tomography. *Inverse Problems*, 28(3):035002, 2012.

- [32] L. Kunyansky, C. P. Ingram, and R. S. Witte. Rotational magneto-acousto-electric tomography (MAET): Theory and experimental validation. *Physics in Medicine & Biology*, 62(8):3025–3050, 2017.
- [33] L. Kunyansky, E. McDugald, and B. Shearer. Weighted Radon transforms of vector fields, with applications to magnetoacoustoelectric tomography. *Inverse Problems*, 39(6):065014, 2023.
- [34] G. M. Lieberman. *Oblique Derivative Problems for Elliptic Equations*. World Scientific, Singapore, 2013.
- [35] H. Liu and G. Uhlmann. Determining both sound speed and internal source in thermo- and photo-acoustic tomography. *Inverse Problems*, 31(10):105005, 2015.
- [36] L. Qiu and F. Santosa. Analysis of the magnetoacoustic tomography with magnetic induction. *SIAM Journal on Imaging Sciences*, 8(3):2070–2086, 2015.
- [37] L. Qiu and S. Zheng. Lipschitz stability of recovering the conductivity from internal current densities. *Inverse Problems*, 39(8):085010, 2023.
- [38] B. J. Roth and K. Schalte. Ultrasonically-induced Lorentz force tomography. *Medical & Biological Engineering & Computing*, 47(6):573–577, 2009.
- [39] P. Stefanov and G. Uhlmann. Thermoacoustic tomography with variable sound speed. *Inverse Problems*, 25(7):075011, 2009.
- [40] A. M. Stewart. Longitudinal and transverse components of a vector field. *Sri Lankan Journal of Physics*, 12:33–42, 2011.
- [41] P. P. Tarjan and R. McFee. Electrodeless measurements of the effective resistivity of the human torso and head by magnetic induction. *IEEE Transactions on Biomedical Engineering*, BME-15(4):266–278, 1968.
- [42] A. Ö. Tetik and N. G. Gençer. MAET with magnetic field measurements using circular and figure-of-eight coils. In *2023 IEEE Biomedical Circuits and Systems Conference (BioCAS)*, pages 1–5, 2023.
- [43] G. Uhlmann. Electrical impedance tomography and Calderón’s problem. *Inverse Problems*, 25(12):123011, 2009.
- [44] H. Wen, J. Shah, and R. S. Balaban. Hall effect imaging. *IEEE Transactions on Biomedical Engineering*, 45(1):119–124, 1998.
- [45] T. Widlak and O. Scherzer. Hybrid tomography for conductivity imaging. *Inverse Problems*, 28(8):084008, 2012.
- [46] R. Zengin. *Electrical Impedance Tomography Using Lorentz Fields*. PhD thesis, Middle East Technical University, 2012.
- [47] R. Zengin and N. G. Gençer. Lorentz force electrical impedance tomography using magnetic field measurements. *Physics in Medicine & Biology*, 61(16):5887–5905, 2016.